UC Irvine
UC Irvine Previously Published Works

Title
Atomic Force Microscopy Investigation of Human Immunodeficiency Virus (HIV) and HIV-Infected Lymphocytes

Permalink
https://escholarship.org/uc/item/8bx0c7nd

Journal
Journal of Virology, 77(22)

ISSN
0022-538X

Authors
Kuznetsov, YG
Victoria, JG
Robinson, WE
et al.

Publication Date
2003-11-15

DOI
10.1128/jvi.77.22.11896-11909.2003

Copyright Information
This work is made available under the terms of a Creative Commons Attribution License, availalbe at https://creativecommons.org/licenses/by/4.0/

Peer reviewed

eScholarship.org Powered by the California Digital Library
University of California

JOURNAL OF VIROLOGY, Nov. 2003, p. 11896–11909 Vol. 77, No. 22
0022-538X/03/$08.00+0 DOI: 10.1128/JVI.77.22.11896–11909.2003
Copyright © 2003, American Society for Microbiology. All Rights Reserved.

Atomic Force Microscopy Investigation of Human Immunodeficiency Virus (HIV) and HIV-Infected Lymphocytes

Y. G. Kuznetsov,[1] J. G. Victoria,[2] W. E. Robinson, Jr.,[2,3] and A. McPherson[1]*

Department of Molecular Biology and Biochemistry,[1] Department of Microbiology and Molecular Genetics,[2] and Department of Pathology,[3] University of California—Irvine, Irvine, California 92697-3900

Received 15 May 2003/Accepted 18 August 2003

Isolated human immunodeficiency virus (HIV) and HIV-infected human lymphocytes in culture have been imaged for the first time by atomic force microscopy (AFM). Purified virus particles spread on glass substrates are roughly spherical, reasonably uniform, though pleomorphic in appearance, and have diameters of about 120 nm. Similar particles are also seen on infected cell surfaces, but morphologies and sizes are considerably more varied, possibly a reflection of the budding process. The surfaces of HIV particles exhibit "tufts" of protein, presumably gp120, which do not physically resemble spikes. The protein tufts, which number about 100 per particle, have average diameters of about 200 Å, but with a large variance. They likely consist of arbitrary associations of small numbers of gp120 monomers on the surface. In examining several hundred virus particles, we found no evidence that the gp120 monomers form threefold symmetric trimers. Although >95% of HIV-infected H9 lymphocytic cells were producing HIV antigens by immunofluorescent assay, most lymphocytes displayed few or no virus on their surfaces, while others were almost covered by a hundred or more viruses, suggesting a dependence on cell cycle or physiology. HIV-infected cells treated with a viral protease inhibitor and their progeny viruses were also imaged by AFM and were indistinguishable from untreated virions. Isolated HIV virions were disrupted by exposure to mild neutral detergents (Tween 20 and CHAPS) at concentrations from 0.25 to 2.0%. Among the products observed were intact virions, the remnants of completely degraded virions, and partially disrupted particles that lacked sectors of surface proteins as well as virions that were split or broken open to reveal their empty interiors. Capsids containing nucleic acid were not seen, suggesting that the capsids were even more fragile than the envelope and were totally degraded and lost. From these images, a good estimate of the thickness of the envelope protein-membrane-matrix protein outer shell of the virion was obtained. Treatment with even low concentrations (<0.1%) of sodium dodecyl sulfate completely destroyed all virions but produced many interesting products, including aggregates of viral proteins with strands of nucleic acid.

Current models for the human immunodeficiency virus (HIV) virion, based on that of Bolognesi et al. (4), have been discussed in detail (6, 10, 16, 64, 70) and will not be further reviewed. Some points, however, are particularly relevant to the work presented here.

The mature virion contains a cone-shaped protein capsid that is probably not based on strict icosahedral symmetry (50) but on a derivative pattern using a conical hexagonal lattice (18). The conical capsid encapsidates two strands of genomic RNA, each of about 9 kb. Also enclosed in the capsid are molecules of replication enzymes, tRNAs (30, 31), and other less well-defined cellular proteins, such as cyclophilin A (52) and Tsg101 (12). The capsid, or core, of the particle is enclosed within a membrane which is studded with envelope glycoprotein composed of gp120 heads which are noncovalently linked to embedded gp41 transmembrane stalks. Between the core and the lipid membrane is a layer of matrix protein and some accessory proteins as well. The matrix protein is attached to the inside of the membrane through embedded myristyl groups (26, 58) and by electrostatic interactions with lipid head groups (11) which may target virion assembly. Indeed, over 90% of myristoylated Gag is found within lipid rafts (51, 63). Thus, a contiguous assembly of envelope protein-lipid membrane-matrix protein forms a dense shroud about the core. The model for the mature virion is still speculative, as pointed out by Coffin et al. (10), though its features have been increasingly refined by more recent analyses (6, 18, 73). The X-ray diffraction structures of gp120, gp41, and both the matrix and the capsid proteins have been determined, but in all cases, the structures are for only truncated or severely altered forms of the molecules (8, 27, 38, 45). The entire collection of currently known protein structures from retroviruses has been reviewed by Turner and Summers (64) and Frankel and Young (16). These structures, while of substantial value in their own right, have contributed only sparingly to further delineation of the overall architecture of the mature virion.

The model for the immature virion (10, 17, 70, 73) also remains speculative and is probably a compendium of structural states. Prior to cleavage of the Gag protein by HIV protease, the immature virus is composed of radially oriented copies of the Gag polyprotein that are aligned in sectors to produce local order and paracrystalline arrays (17, 70, 73). These polyproteins are anchored to the lipid membrane at the exterior through the matrix protein domain and at the center of the quasi-micelle by protein-RNA interactions mediated by the nucleocapsid domain (6, 73). The aligned copies of the Gag protein, of which there are estimated to be about 2,100 (6, 53),

* Corresponding author. Mailing address: Department of Molecular Biology and Biochemistry, University of California—Irvine, Irvine, CA 92697-3900. Phone: (949) 824-1931. Fax: (949) 824-1954. E-mail: amcphers@uci.edu.

are subsequently cleaved to produce the layered arrangement of the structural proteins, including the conical core (18). The physical process by which this occurs in the interior of the maturing virion is largely unknown.

To this point, transmission electron microscopy (TEM) has been virtually the only source of images of HIV virions and HIV-infected cells, though scanning electron microscopy images have also been recorded at relatively low resolutions (28, 54). Cross sections of cells which have been embedded, stained, and visualized with TEM show the presence of virions near and at cell surfaces in the processes of maturation and budding (10, 21, 23, 68). Those images are revealing and quite remarkable, but they do have certain limitations. First, the cells have been embedded in plastic and later exposed to a heavy metal stain, either or both of which might introduce distortions into the cell and virion structures. In addition, one in fact sees only the pattern of stain from which structure must be inferred. The cells are usually compacted within a centrifuge pellet so that many cells are sectioned at oblique and arbitrary angles. It is virtually impossible to reconstruct and visualize an individual cell in its entirety. While lateral resolution with TEM is potentially high, determining the height, or third dimension, for nonsymmetric objects is problematic. Finally, TEM yields a projection image in which the entire stain distribution throughout and around the specimen is projected onto a single plane. Hence, superposition of components complicates and hinders interpretation of structure.

More recently, cryo-electron microscopy has been used to visualize both immature and mature retroviruses isolated from culture medium (6, 17, 70, 73) as well as isolated HIV capsids (6, 18, 33). These studies, though technically more demanding, are free of many of the artifacts introduced by staining and dehydration and have been quite revealing. Cryo-electron microscopy does, however, still suffer from problems in interpretation due to superposition of features.

Atomic force microscopy (AFM) has both virtues and limitations as well, but they tend to be complementary to those of TEM and cryo-electron microscopy. With AFM, samples may be imaged in air or in fluids, including culture medium or buffer, in situ, or after processing according to established histological procedures (7, 34, 48). AFM is nondestructive and nonperturbing, and it can be applied to soft biological samples, particularly when tapping mode scanning is employed (24, 62). For AFM investigation, in principle, a single cell or virion is all that is required, though several hundred of either may be present on the substrate. An isolated cell or virion may be imaged in its entirety, or many individuals may be examined. While lateral resolution, limited by the finite size of the cantilever tip, is only 5 to 10 nm, the height resolution is very good, better than half a nanometer. Finally, AFM produces three-dimensional, topological images that accurately depict the surface features of the object under study. In most ways, these images resemble common light photographic images.

We have shown in previous investigations of viruses by AFM that the technique is sufficiently incisive and reproducible that even individual capsomeres can be visualized on the surfaces of both plant and animal viruses. Furthermore, it has been shown that the structures of viruses observed by AFM are entirely consistent with models derived by X-ray crystallography and cryo-electron microscopy (1, 35, 37, 42, 43, 55). In a recent paper, we showed that AFM was a valuable approach for visualizing a similar retrovirus, murine leukemia virus (MuLV). For that investigation, both isolated virions free on glass substrates and virions emerging from infected cell surfaces were imaged by AFM, as were mutant viruses which formed aberrant virions (34). Here, we extend our AFM studies to HIV and HIV-infected lymphocytes.

MATERIALS AND METHODS

Cells and viruses. H9 cells, a $CD4^+$ human T-lymphoblastoid cell line, were cultured in growth medium (RPMI 1640) containing HEPES and 2 mM L-glutamine supplemented with 11.5% heat-inactivated fetal bovine serum. Cells were reduced by half and refed every other day. HIV_{LAI} was obtained from the NIH AIDS Research and Reference Reagent Program. H9 cells chronically infected with HIV_{LAI} and 100% positive for virus antigens by immunofluorescence assay (32, 59) served as the source for HIV and HIV-infected cells. Briefly, cells were air dried and fixed to glass slides. Cells were incubated first with a gamma globulin fraction pooled from HIV-infected individuals, followed by fluorescein-conjugated goat anti-human immunoglobulin G (IgG). Antigen-positive and -negative cells were counted with a Nikon epifluorescent microscope. Images were made by use of a SPOT Insight charge-coupled device camera.

Preparation of virus and cells for AFM imaging. Cells were cultured for 48 h at 37°C, and supernatant fluids were clarified of cells by low-speed centrifugation followed by filtration through 0.45-μm-pore-size cellulose acetate filters. Ten milliliters of filtered supernatant was centrifuged at 25°C for 4 h at 30,000 × *g*. Pelleted virus was resuspended in 40 μl of RPMI 1640 and allowed to adhere to poly-L-lysine (50 μg/ml)-coated glass coverslips (Sigma) for 18 h at 37°C. Coverslips were rinsed with 5 ml of phosphate-buffered saline (PBS) and then incubated with 0.1% glutaraldehyde for 30 min followed by 1.0% osmium tetroxide incubation for 30 min. Fixed HIV was dehydrated and inactivated by washing with 30, 50, and 70% solutions of ethanol for 7 min each. For imaging of uninfected and HIV-infected cells, approximately 10,000 nonadherent HIV-infected or uninfected H9 cells were layered onto poly-L-lysine-coated coverslips at a concentration of 100,000 cells/ml and allowed to adhere at 37°C in RPMI containing 11.5% fetal bovine serum for 18 h. Adherent cells were fixed and dehydrated essentially as described for HIV virions.

Virion lysis by nonionic and ionic detergents and drug treatment. For some experiments, HIV was disrupted by use of nonionic detergents prior to AFM imaging. Before glutaraldehyde fixation, HIV which had adhered to coverslips was exposed to various concentrations of detergents (0.10 and 0.5% Tween 20, 0.5 and 2% CHAPS, or 0.1 to 2% sodium dodecyl sulfate [SDS]) for 5 min and then washed twice with PBS. For other experiments, to determine whether virion morphology was altered in immature versus mature HIV, HIV_{LAI} was produced in the presence of nelfinavir, an HIV protease inhibitor. HIV_{LAI}-infected H9 cells were cultured in the presence of 4 μM nelfinavir, and supernatants were cleared of mature virions after 5 h by low-speed centrifugation of cells, which were then washed with PBS. Cells were resuspended in medium containing 4 μM nelfinavir and incubated for 48 h at 37°C. HIV was pelleted and processed for AFM as described above.

AFM. AFM instruments and procedures have been previously described for application to both cells (37) and viruses (36). Before imaging, fixed cells were dehydrated by washing the fluid cell with 30, 50, and 70% solutions of ethanol for 7 min each. Treatment with ethanol removes the lipids from the membranes of both cells and virions but leaves behind skeletal proteins of the membranes (2, 25) when fixation is done with glutaraldehyde alone. The use of osmium tetroxide postfixation, however, cross-links membrane lipids as well as proteins, and the lipids are therefore not removed by alcohol exposure. This additionally preserves many, if not all, membrane-associated proteins as well. After fixation, coverslips were washed with H_2O and attached to metallic packs with double-sided tape. Coverslips were mounted on a J-piezoscanner of an atomic force microscope equipped with a fluid cell (Nanoscope III; Digital Instruments, Santa Barbara, Calif.).

Cantilevers with oxide-sharpened silicon nitride tips were 100 μm long. Images were collected in tapping height mode at frequencies of about 9.2 kHz, with a scanning frequency of 1 Hz. Because of the finite tip dimensions, isolated objects protruding above the background in AFM images appear broader than their true dimensions. For this reason, the dimensions of virions and their components were quantitated according to their heights above the background surface (36). Estimates of particle size given here are based on images obtained by height measurement of 100 to 200 particles on either glass substrates or on cell surfaces.

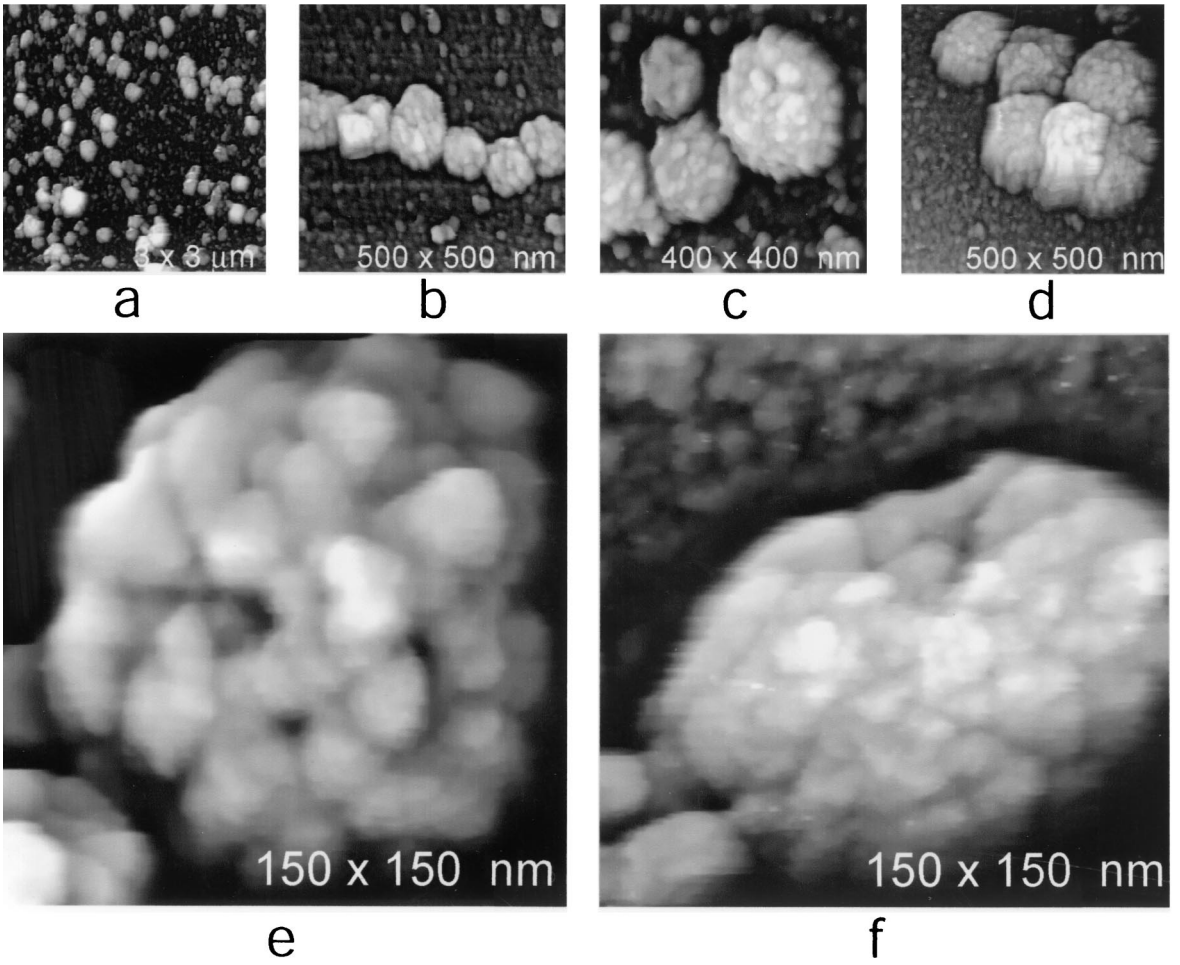

FIG. 1. Isolated HIV particles. AFM images of particles obtained by centrifugation of the culture medium from an HIV-infected cultured human lymphocytic cell line are shown. The resuspended virions were spread on poly-L-lysine-coated glass coverslips, fixed with 0.1% glutaraldehyde and 1.0% osmium tetroxide, and imaged by AFM under ethanol. (a to d) Groups of virus particles adhering to the glass substrate. The tendency to form clusters is likely due to packing of particles as a result of centrifugation. (e and f) Two isolated viruses imaged at high resolution showing the distinctive but arbitrary distribution of protein tufts covering their exterior surfaces. The roughly spherical particles have average heights of 120 nm, although some, as in panel f, are seen to be slightly compressed, probably due to contact with the substrate. The particles appear to be soft and easily deformed from a spherical shape. The images seen here are typical of many such particles found on the substrate.

There is no evidence that the mild fixation with glutaraldehyde used here appreciably disturbs the structures of the cell and virus surfaces, at least to the resolution of these AFM studies. For example, we and others have fixed numerous protein and virus crystals with the same low concentrations of glutaraldehyde, and these crystals show no loss of resolution, increased mosaicism, or change in X-ray diffraction intensity distribution. We also, in previous studies (36), examined plant virus crystals under ethanol (even without glutaraldehyde fixation) and saw no obvious alteration in their surface structures compared to X-ray crystallography-determined structures, again to the resolution of the AFM images.

Direct evaluation of shrinkage of HIV due to fixation and/or dehydration was not possible for safety reasons, but extensive experiments using MuLV as a standard particle showed that fixation under our conditions produced no effect on dimensions. The same experiments in which particles were imaged in both water and ethanol, however, showed that dehydration of fixed virions, while not altering topological features, reproducibly resulted in a reduction in dimensions of 15% ± 2%. The particle sizes reported here have been corrected for shrinkage.

In the images presented here, the features are assigned a color indicative of their height above the substrate; hence, dark colors show very short (close to the substrate plane) features and light colors represent tall features, that is, features protruding above the substrate plane. White areas or points are features that are very high above the substrate plane in comparison to all other features on the object surface. It is important to bear in mind that AFM does not yield two-dimensional projections of objects onto a plane, as does TEM or light microscopy. Because height information is recorded as a function of a coordinate, a three-dimensional, topologically precise image is obtained of objects.

RESULTS

Virions from culture medium. Virions were routinely prepared, as described above, by centrifugation of HIV-infected H9 cell cultures and were spread on poly-L-lysine-coated glass coverslips for examination. Figure 1 presents an array of typical examples of HIV virions as revealed by AFM. When culture medium from equivalent cells that were not infected with HIV was used, no particles resembling these were observed (not shown). The particles are roughly spherical and have a crenulated, pleomorphic exterior characterized by a dense packing of protruding protein units. Though the appearances of the virions were more or less uniform, their diameters varied

by 25 nm about an average of 120 nm (based on height measurement of 300 particles). The particle size we report here is somewhat smaller than that determined by both negative-staining TEM (10, 68) and cryo-electron microscopy (6). In the latter investigation, the diameter of particles containing a single core was estimated to be about 134 ± 11 nm.

The variation in virion size about the mode of the distribution is real, and it is not due to measurement error, which is no more than 5 nm for each particle. This average diameter is about 5 nm less than that we find for the virions on cell surfaces (see below). We do not believe that this size difference is a consequence of physical change in the virus upon release from cells but that it more likely reflects loss of surface proteins and some slight compression upon centrifugation. Centrifugation is known to strip surface proteins from retroviral particles and, indeed, we also see some virions on the substrate that appear broken or damaged. We assumed the virions purified from the medium which had diameters somewhat greater than the average to be the most intact and best representatives of native HIV.

Among the particles displayed on the glass substrate were some that were much smaller, on the order of 80 to 100 nm in diameter, and some that were much larger, on the order of 160 to 240 nm in diameter. These particles were not included in the averaging and were taken to be aberrant particles, the former likely lacking cores and the latter perhaps having multiple cores. Indeed, virions containing multiple cores have been reported by Gelderblom (20) and estimated by Briggs et al. (6) to comprise as much as 30% of the entire virus population based on cryo-electron microscopy. In addition, Briggs et al. (6) report that as many as 7% of HIV virions contain not conical but tubular cores, and these might also contribute to the variation in shape and size that we observe for virions by AFM. Qualitatively at least, the distribution of particle sizes that we observe is in good agreement with that reported by Briggs et al. (6).

The particles recovered from the medium and displayed on the glass substrate appear almost identical to those visualized on the surfaces of HIV-infected cells and are virtually indistinguishable from virions of MuLV imaged in an earlier study (34). It is also relevant to experiments described below that the background of cell and virus debris on the glass substrates, particularly protein, was remarkably low. Preparations of virus particles and the AFM images obtained, though somewhat dependent on the properties of individual AFM tips, were otherwise reproducible.

AFM of uninfected and infected cultured lymphocytes. H9 cells, both uninfected and infected with HIV, were similarly applied to poly-L-lysine-coated glass coverslips and visualized by AFM. The uninfected H9 cells were negative for HIV antigens (Fig. 2A), while essentially 100% of the HIV-infected cells were positive for HIV antigens (Fig. 2B) by immunofluorescence assay. AFM images of uninfected human lymphocytes taken from culture are shown in Fig. 3. In contrast to most other cells we have examined, such as fibroblasts and osteoclasts (37), the surfaces of both patient-isolated peripheral blood lymphocytes (data not shown) and lymphocyte cell lines tend to be far more complex. They are heavily decorated with protrusions of all sizes, microvilli, and membranous structures having a variety of forms. This is consistent with previous investigations on antigen-activated NK cells which show "numerous ruffled cell membrane projections" (5) and others describing complex microvilli formation and severe morphological changes of isolated lymphocytes (14). No two cells closely resemble one another, and there is a broad distribution of cell sizes, ranging from about 5 to 15 μm. It is consistent, as well, with results from scanning electron microscopy, yielding sizes of 8 to 10 μm (60), or with scanning AFM, yielding a size of 15 μm (49), along with varying cell shapes and surface features. This may reflect different stages of the cell cycle or different physiological states of individual cells. No particles resembling the virions seen in Fig. 1 were observed on the surfaces of uninfected cells.

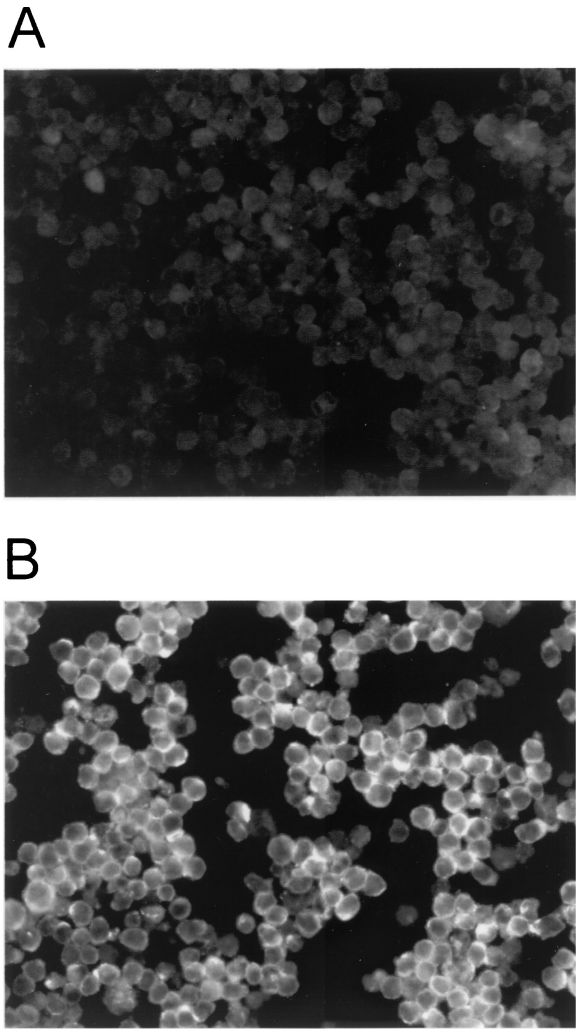

FIG. 2. Immunofluorescence assay for H9 (A) and HIV-infected H9 (B) cells. Cells were dried, fixed on glass slides, and incubated first with an IgG fraction from HIV-infected individuals and then with fluorescein-conjugated goat anti-human IgG. Both antigen-positive and antigen-negative cells were observed and counted to determine the percentage of HIV antigen-positive cells. Images were captured with a SPOT Insight charge-coupled device camera.

HIV-infected cells exhibited striking diversity in the number of virus particles present. In most cases, one or only a few virus particles were visible on infected cells, and often none were

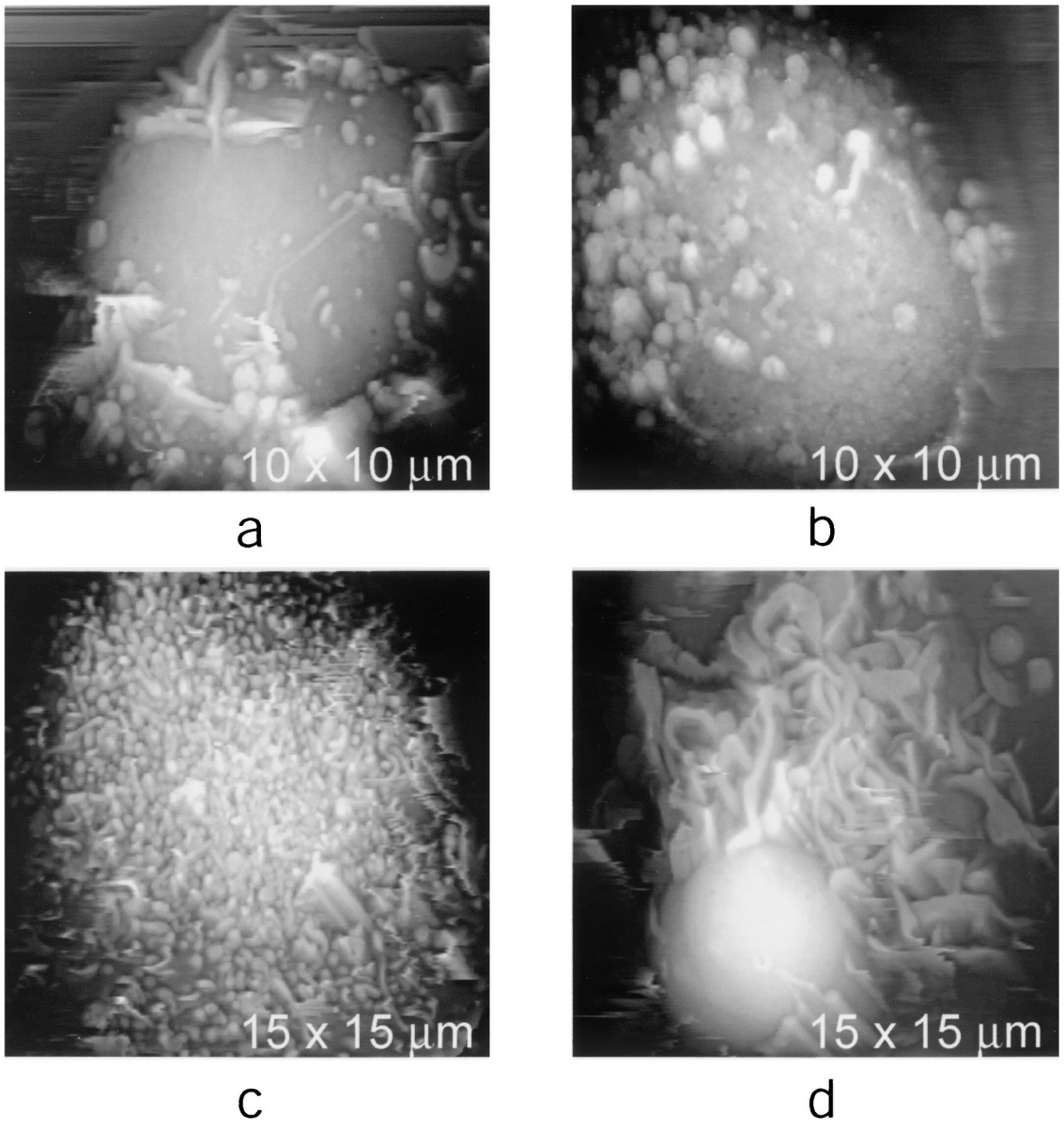

FIG. 3. Uninfected human lymphocytes. AFM images of an uninfected human lymphocytic cell line in culture showing the remarkable diversity of their external features are shown. In most cases, there are large smooth surfaces combined with a variety of membranous protrusions, microvilli, and films (a and b). Some cells are almost totally covered with microvilli and membranous structures (c and d [higher resolution]). The cell in panel d exhibits a dense accumulation of microvilli along with a smooth, protruding, dome-like feature. These lymphocytes are the most complex and heterogeneous cells that have so far been visualized by AFM.

visible. The same was true for MuLV-infected human fibroblasts (34). An example is the cell shown in Fig. 4a, which exhibits at least six spherical protrusions of approximately 120 nm in size which have morphologies nearly identical to the free viruses seen in Fig. 1. Some cells, however, were literally coated with virus, often exceeding a hundred virions. Examples of such cells are shown in Fig. 4b and c. The highly prolific cells may be unique in their genetic makeup or physiological or developmental state, or they may represent cells unable to fully release progeny viruses, which accumulate over time. The virions are, in these cases, seen both on the smooth portions of the cell surfaces and thoroughly intermixed with the microvilli and membrane structures.

It may be worth noting that the appearance of large swarms of emerging particles crowded closely together was not seen for MuLV-infected fibroblasts (34). MuLV particles appeared more frequently as individuals evenly distributed over cell surfaces. Groups of closely associated virions were rarely seen, and larger masses were not observed.

Some microvilli on infected cells, like those in Fig. 4d, are segmented, and the segments have dimensions corresponding to HIV particle sizes. This suggests that some microvilli may

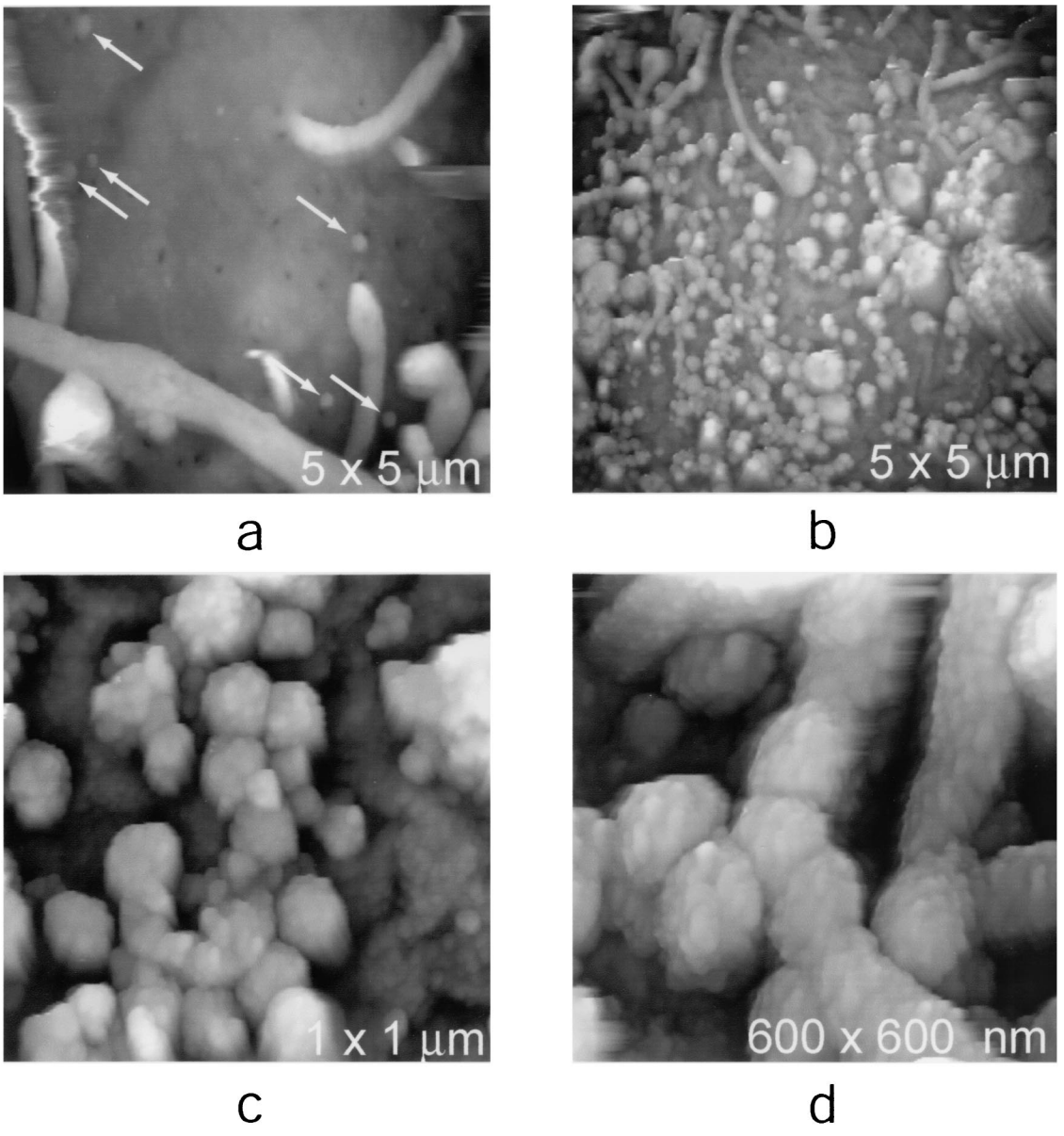

FIG. 4. AFM images of HIV-infected H9 cells. (a) AFM image of an HIV-infected H9 cell. On its surface, marked by arrows, emerging HIV particles can be seen. At high resolution, they have the appearances of those particles seen in Fig. 1. The particles are not present on uninfected cells. This cell appears to have, overall, only 5 to 10 HIV particles on its surface, which is about average for the infected cells. Some cells had fewer particles or none at all. Occasionally, cells were observed which appeared to be virtually covered with viral particles (b). (c) AFM image of a cascade of emerging particles on one such cell. (d) An example of microvilli on the surface of an HIV-infected lymphocyte which exhibits a distinctive segmentation. The sizes of the segments, which in some cases are roughly spherical in shape, are in the range of 120 nm, corresponding to the diameters of virus particles.

contain virus, and they may provide a venue for virus maturation. Viral particles budding through microvilli of infected primary monocytes have previously been shown by scanning electron microscopy and TEM (54). They are not essential, however, as most virions are observed by AFM to be budding directly from the plasma membrane.

Figure 5 is a gallery of HIV virions imaged by AFM as they emerge from, or are attached to, the surfaces of infected cells. Presumably, they represent a mixture of immature and mature particles and possibly virions in intermediate states. The particles have an average diameter of 127 nm, with a variation of 30 nm, based on measurement of 200 particles. Again, the distribution is broad, not because of measurement error, but because of the actual size diversity of the virions. A similar range of size diversity of particle diameters about the mean based on cryo-electron microscopy has been observed by Briggs et al. (6) as well. As with the free particles on a glass substrate, we again observed some particles that were considerably smaller than 127 nm which had the gross appearance of virions. These, we believe, may be particles lacking cores. Also

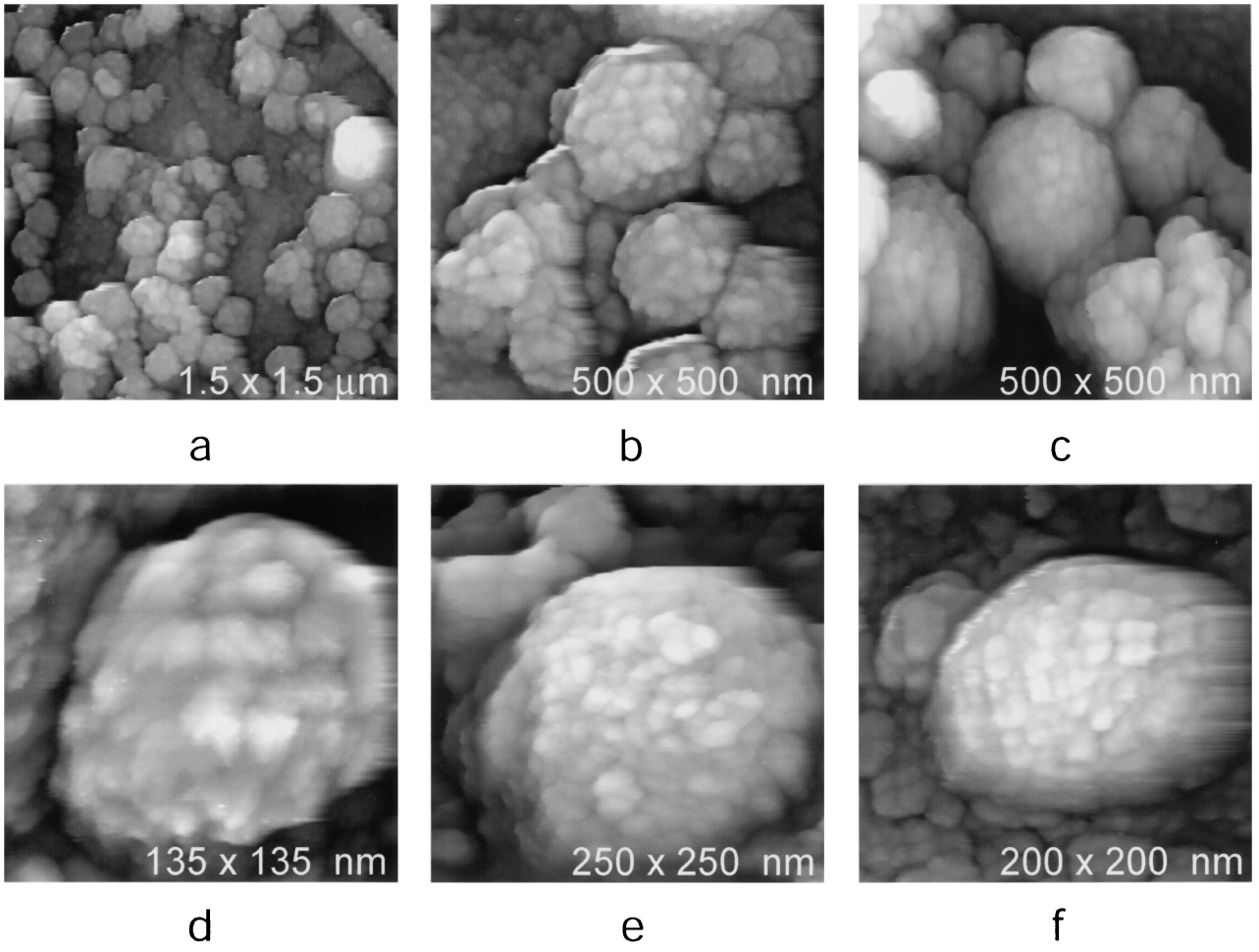

FIG. 5. HIV on cell surfaces. Shown is a gallery of AFM images of HIV particles emerging from or attached to the surfaces of human lymphocytes. The complex virion surfaces vary in detail from particle to particle, suggesting that the clusters of envelope proteins arise from more or less arbitrary associations of subunits. Particles have average diameters of 127 nm and exhibit exteriors similar to those in Fig. 1.

frequently present were some anomalously large particles that otherwise had the appearance of virions. These had diameters in the range of 160 to 240 nm and probably represent virions that contained multiple cores. The external appearances of the virions having diameters of about 127 nm, the vast majority, are similar to one another and are the same as those of the free virions. The larger and smaller particles are usually more irregular in structure.

Disruption of virions by exposure to nonionic detergents. HIV virions spread on glass coverslips were exposed to a wide range of concentrations of mild detergents (Tween 20 and CHAPS) until a concentration was identified in which intact virions, partially disrupted virions, and degradation products were simultaneously present. This we took to be the minimum concentration required to effect particle disruption and still preserve large fragments and other products. The optimal ranges were between 0.1 and 0.50% for Tween 20 and between 0.5 and 2% for CHAPS. This is in the range of concentrations of Triton X-100 used for the disruption of virions and the preparation of intact cores (6, 33).

Figure 6 shows a series of images typical of the many disruption experiments that we carried out. Recognizable HIV virions can be found, but two other products are now also present. These are damaged, split, and broken virus particles in the process of coming apart and a dense background of viral components, presumably the proteins and macromolecular components from more thoroughly degraded virions and virion cores.

Two points are particularly worth noting. First, the heavy background of smaller products must have arisen from disruption of the virions and must represent viral components, because no such background, as noted above, was present prior to the application of detergent. Furthermore, no such background was observed with supernatants from uninfected cells, with or without detergent (data not shown). Second, in viewing many samples, we at no time observed any subparticle that was clearly recognizable as a virus core. One possibility is that our perception of the core based on the existing model is incompatible with the structure as it really exists and another is that the cores of the virions are degraded by a neutral detergent more readily than the envelope lipoprotein complex. The latter explanation is most likely, since it is consistent with other, earlier studies showing that the core structures are even more

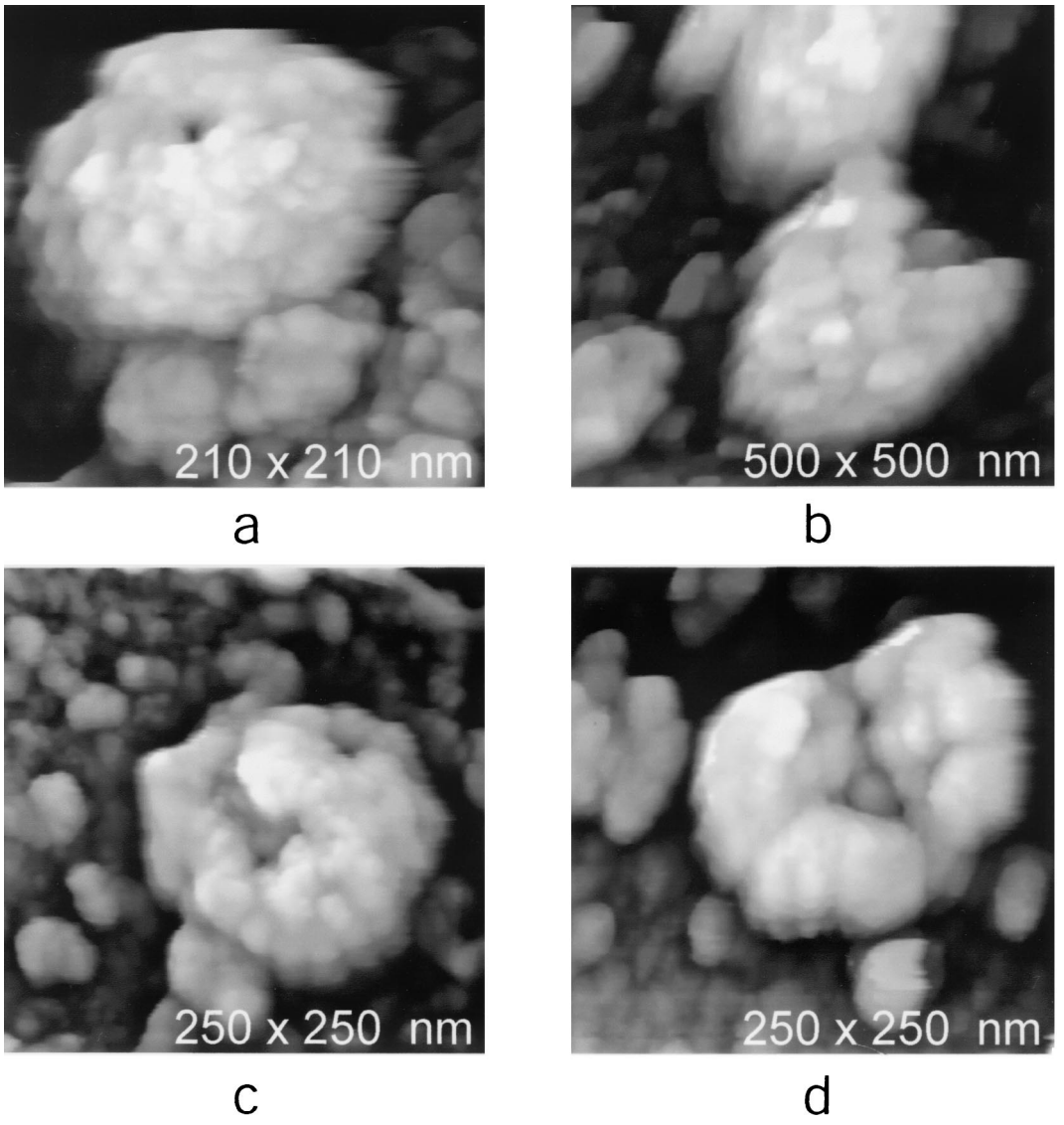

FIG. 6. Detergent-disrupted virions. When HIV virions collected from their media are spread on glass slips and treated with mild detergents, partially degraded or damaged virions are frequent products. (a) Particle with a sector of its surface missing, which leaves a deep pit leading to the interior. Such particles are rarely seen in HIV populations in the absence of detergent treatment. (b to d) More severely disrupted particles. The particle in panel b has a large gaping cavity, and for the one in panel c, the top of the particle appears broken open and exposed. The particle in panel d is completely split open. The view is of the interior surface of the envelope and the cavity once occupied by the capsid. There is also, in all images, a heavy background of fragments, proteins, and viral debris from the disrupted particles.

susceptible to disruption by mild detergents than are the mature, enveloped virions (66).

Examination of the partially disrupted particles is instructive in terms of understanding the organization of the HIV virion. First, particles are often encountered which exhibit a sector of missing protein on their surfaces, and this appears as a deep pit or cavity that penetrates into the interior of the virion. An example is shown in Fig. 6a. A possible explanation for these particles is that they have lost their nucleic acid-containing core through the opening and are now empty virions. Indeed, because of the finite size of the AFM tip, these cavities undoubtedly appear of less severity than is actually the case. Thus, although they may appear rather narrow in the micrographs, they are probably on the order of 40 to 50 nm in width and possibly large enough for a somewhat fluid capsid to pass. Judging from electron micrographs of isolated cores (33), their broad size and shape distributions suggest that the cores may indeed be quite malleable, even fluid, and could potentially escape through openings of the sizes that we observe.

Particles with missing sectors of protein also occur, but with less frequency, in populations of virus that are not treated with detergents and even in some virions seen on the surfaces of HIV-infected cells. Such particles were also observed in our studies of MuLV, and we in fact drew attention to them in our earlier paper (see Fig. 4 of reference 34). There is, we believe, an equally plausible explanation for the particles of HIV and MuLV that exhibit deep pits in their surfaces, like those seen in Fig. 1f and 6a. The envelope is formed by budding from the

plasma membrane of the host cell and targeted to lipid rafts (40), which are estimated to be about 50 nm in diameter (57, 61, 65). The current model of viral budding involves binding of the 4-amino-acid Gag p6 PTAP motif to cellular Tsg101 protein and subsequent assortment via the cellular vacuolar protein-sorting pathway (13, 19, 44, 56). Pinching off the viral membrane from the host cell membrane is an ATP-dependent process which may generate a concentrated ring of both cellular and viral proteins. This pinch point, or budding scar, may repair seamlessly and components may redistribute so that no structural vestige remains on the envelope, i.e., the virion surface becomes spherically homogeneous. On the other hand, budding may result in an asymmetric distribution of proteins on the virion surface, making the point of budding more susceptible to disruption by detergents. This model is additionally consistent with particles exhibiting missing sectors, even in the absence of detergent, if the sealing process is at least occasionally imperfect.

Images of other virions were recorded that were at later stages of disruption and that had lost their interior cores completely. Examples are shown in Fig. 6b to d. Note that the virus particles do not appear to fall apart one subunit or sector at a time or bit by bit (as observed in a study of herpesvirus [55]), but they split or break like a fruit or nut, leaving behind thick "husks" or "peels" and an empty central cavity.

The remnant husks permit measurement of the thickness of the envelope of the virion surrounding the core. From the AFM images, these husks are about 35 nm thick. The cavity is about 40 to 50 nm in diameter, consistent with the reported size of the core (6, 18, 29). The thickness of the envelope is explicable only if we assume that it consists of a contiguous assembly of envelope protein, lipid membrane, and matrix protein. Indeed, this is reasonable since the gp41 envelope glycoprotein is known to be firmly embedded in the membrane on the outside, and the matrix protein is affixed to the same membrane on the inside through its myristyl modifications. There is even evidence, in fact, that the transmembrane portion of the envelope protein, gp41, may directly associate with the matrix protein through its cytoplasmic tail (72), thus creating a contiguous polypeptide linkage. Thus, the entire assembly forms a single thick-walled protective envelope for the apparently fragile, mobile, and perhaps even fluid core. Such a structure is consistent with the observation of Wilk et al. (70) that the matrix protein appears by cryo-electron microscopy to be a thin layer tightly associated with the inner face of the viral membrane.

Disruption of virions with ionic detergents. Use of high concentrations of the neutral detergent Tween 20, in the range of 2% or greater, produced complete destruction of the virions and left large amounts of macromolecular components and their aggregates on the substrate. We could, however, find no recognizable traces of the nucleic acid. Concluding that the neutral detergent was simply inadequate to completely dissociate protein-RNA complexes and reveal the nucleic acid, we explored the exposure of virions to SDS, a strong ionic detergent.

At concentrations of SDS of >0.1%, virions were disrupted completely and none were present on the substrate, although large aggregates of viral components were again observed. At high concentrations (>0.5%) of SDS, however, the aggregates were largely dissociated, and threads, often heavily decorated with residual proteins, became visible by AFM. Some examples are shown in Fig. 7. These are consistent in appearance with previous AFM observations of extended nucleic acid-protein complexes from other viruses, such as tobacco mosaic virus and cauliflower mosaic virus (36), herpes simplex virus (55), and vaccinia virus (43). These chains of protein molecules, linked together by the nucleic acid, are characteristic and readily identified. It is significant that simple repetitive nucleoprotein chains were not seen, but chains having large proteins or protein complexes of a variety of sizes bound to them, possibly representing not only nucleocapsid proteins but also larger replicative enzymes and enzyme complexes. The resistance of the protein-nucleic acid complexes to strong detergents suggests that the components of the complexes are indeed tightly bound to one another.

Protease inhibitor-treated HIV-infected cells and virions. Imaging of protease inhibitor-treated, HIV-infected cells by AFM showed no difference in the numbers of cells expressing virus or in the distribution of virions on the cell surfaces. This is consistent with fluorescence microscopy observations of the same cells which indicate virtually all to be HIV infected. Previous studies have demonstrated marked differences between immature and mature viral core particles by use of TEM (28) and between densities, as measured by sucrose equilibrium gradients (39). Additionally, virus-like particles (VLPs) generated by baculovirus expression of Gag proteins display striking changes between unprocessed Gag VLPs, which contain a doughnut-like shape, and processed, mature VLPs (47). More recent studies using cryo-electron microscopy further demonstrate dramatic differences in the internal structures of immature and mature virions (6, 17, 70, 73). Those same studies, however, also indicate that there are no perceptible changes in either the sizes of the particles or their exterior features. Despite dramatic changes in the internal core of the virus, the surfaces of the viruses as imaged by AFM (Fig. 8a to d), consistent with the studies cited above, were indistinguishable from those of virions expressed by untreated cells in terms of size distribution, average size, and surface properties. These virions showed the same pleomorphic, tufted appearance as those from untreated cells. The same was true of virions from protease inhibitor-treated cells collected by centrifugation from the medium, like those shown in Fig. 8e and f. This underscores both the inherent differences and the complementary nature of AFM and TEM. While electron microscopy reveals radical alterations of viral core structure between mature and immature viruses that cannot be observed by AFM, AFM demonstrates a uniform surface during maturation that cannot be visualized by electron microscopy.

DISCUSSION

The AFM results that we report here are generally consistent with the currently accepted model for the mature retrovirus virion (4, 6, 10, 64, 73). At a more detailed level, however, there are some disagreements, particularly with the portion of the virion which surrounds the core. A principal discrepancy involves the surface of the virion and the arrangement of the gp120 and gp41 envelope proteins (discussed in the work of Wyatt and Sodroski [71]).

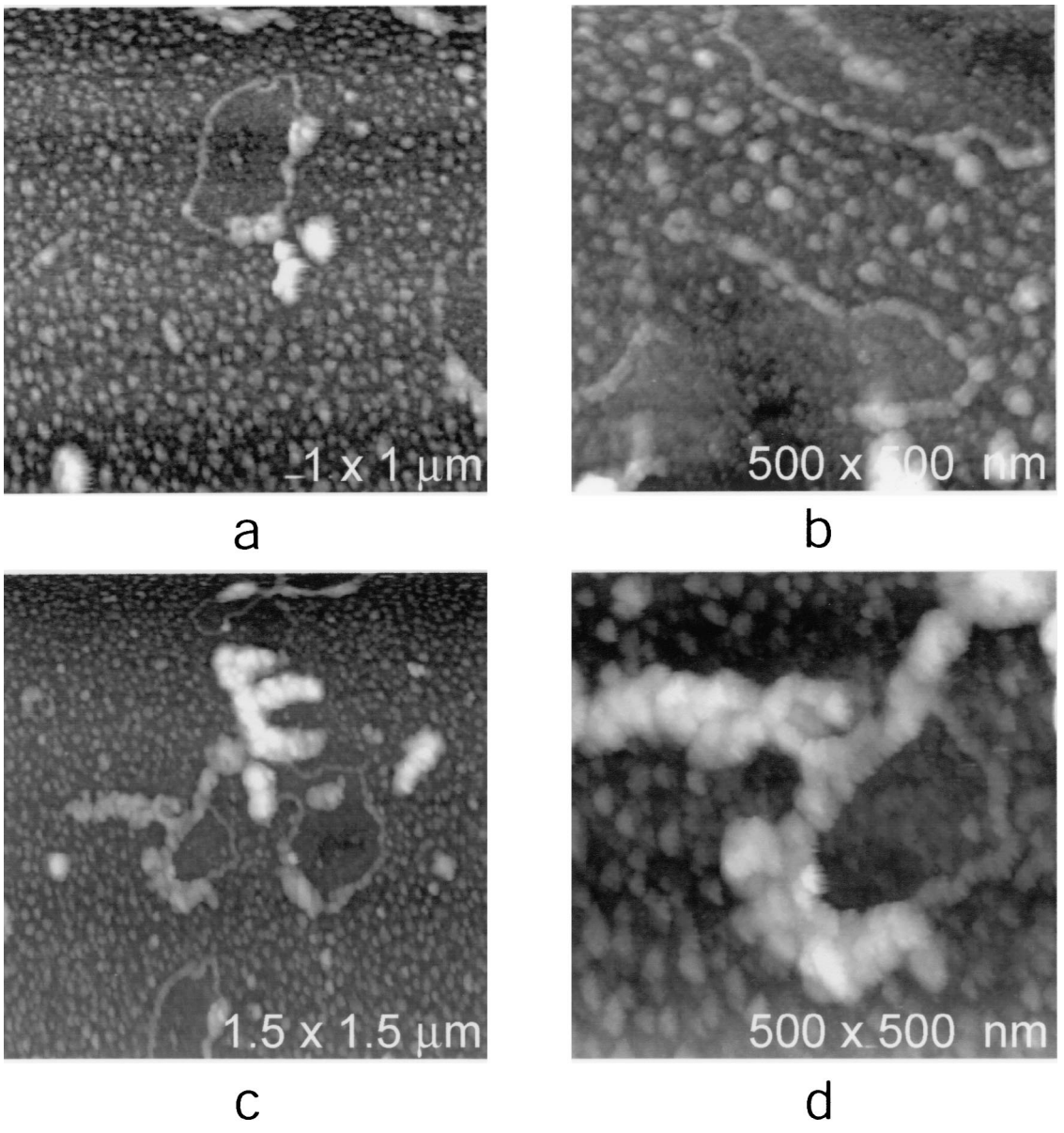

FIG. 7. Protein-nucleic acid complexes. HIV virions disrupted by incubation with 0.5% SDS, a strong detergent, are shown. When HIV virions spread on glass are disrupted with a strong detergent, nearly complete degradation occurs and elements of the nucleic acid, almost always associated with proteins and protein aggregates, are a major product.

The surface of HIV is comprised of the receptor binding protein gp120, which is, in turn, noncovalently connected to the lipid membrane by the protein gp41. The structure of a truncated form of the transmembrane gp41 is known from X-ray crystallography (8, 67), and in the crystal is a threefold symmetrical coiled-coil trimer of six long α-helices. The structure of a core portion of gp120, lacking several external polypeptide loops and 90% deglycosylated, has also been solved by crystallography (38), as has the homologous protein from MuLV (15). gp120 is commonly assumed to be a symmetrical trimer, principally due to its association with the trimeric gp41, but that has, in fact, never been demonstrated. On the other hand, the envelope protein of human foamy virus (HFV) has convincingly been demonstrated to be a threefold symmetrical trimer by cryo-electron microscopy, both in its free form and when it is a part of the virion (70). By homology, therefore, one might reasonably expect the corresponding proteins of other retroviruses to have the same oligomeric structure.

The prominent tufts forming the surfaces of HIV particles in the AFM images must, according to their sizes, be aggregates of gp120. We have examined many hundreds of these tufts on many hundreds of particles and have found no evidence of even approximate threefold symmetry. The variation in size and shape of the tufts suggests that in the native HIV particle, gp120 forms surface clusters; however, they do not exist as closely associated symmetrical groups but in more arbitrary and varied arrangements.

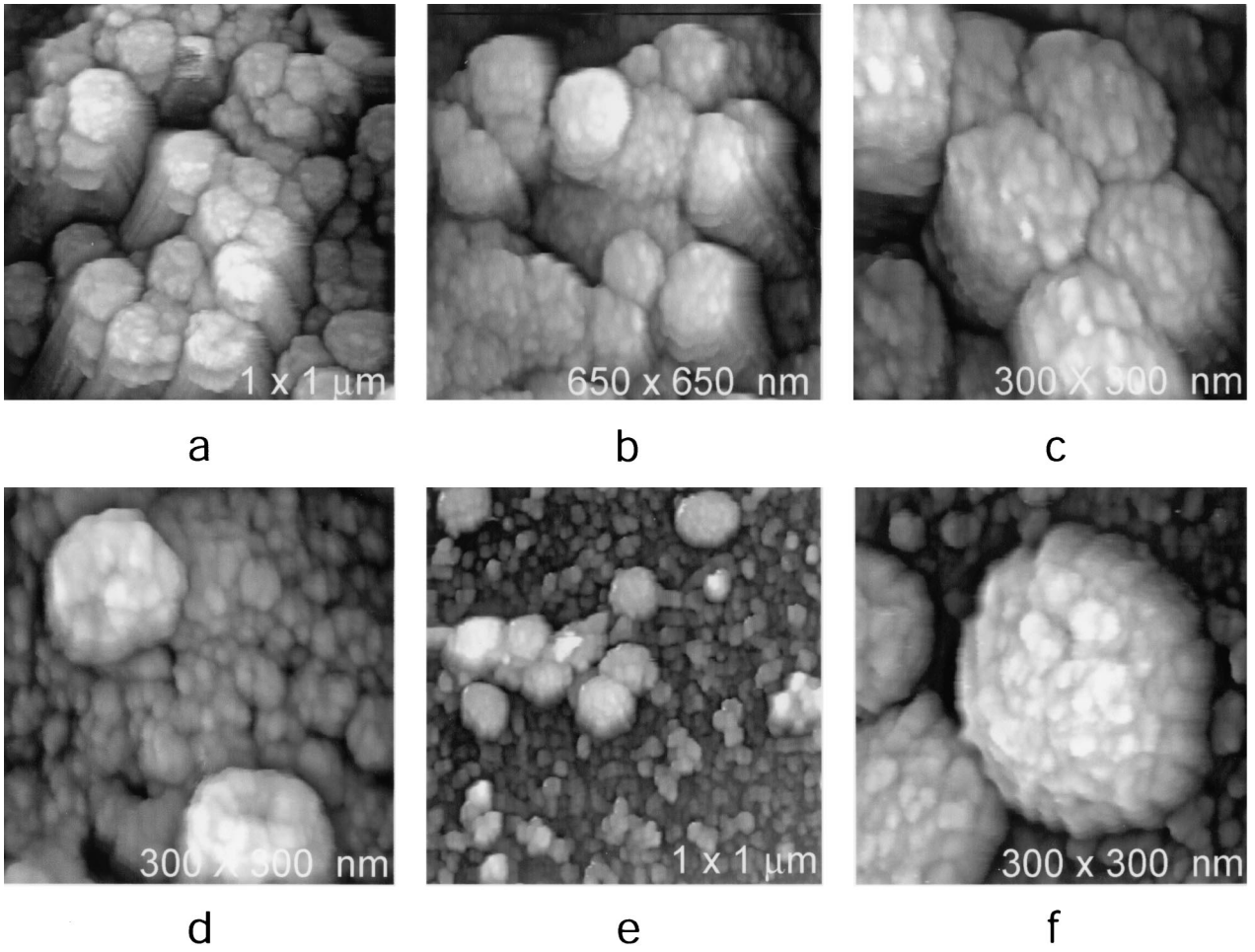

FIG. 8. Protease inhibitor-treated cells. (a to d) Infected cells treated with the protease inhibitor nelfinavir. The particles are not perceptibly different in surface character from those on untreated cells. (e and f) Particles collected from the medium of HIV-infected cells treated with the protease inhibitor nelfinavir. These virions also look quite similar to normal HIV particles in size and shape.

The gp120 clusters are also inconsistent in terms of average size with symmetrical trimers. Their average diameter of about 200 ± 30 Å is significantly greater than that which might be expected for a trimer of 360 kDa. The surface area subtended by a cluster is more than twice as great. In addition, the tufts are not of consistent diameters but vary among themselves by about 30 Å or more. While the heavy glycosylation may contribute to both of these features, it is unlikely to entirely explain either. It seems probable that the individual gp120 monomers at the ends of gp41 stems, like heads of flowers in a bouquet, are otherwise separated from one another and make no systematic protein-protein contacts. Associations are arbitrary with neighbors, and the groupings therefore exhibit no consistent symmetry or shape.

A disordered arrangement of unliganded gp120 monomers is consistent with their unusually flexible and mobile character, their existence in multiple conformation states (38, 71), their conformational changes on binding ligands, such as CD4 (38, 46, 71), and their heavy coatings of oligosaccharides, which would tend to impede direct contact between polypeptide chains. It is supported, as well, by the observation that recombinant gp120, when expressed in insect cells, remains monomeric and does not crystallize as trimers (38), and neither does the homologous SU envelope protein from MuLV (15).

Aside from an anticipated structural homology with the envelope protein of HFV, the primary evidence suggesting that gp120 monomers form symmetric trimers on the surfaces of HIV stems from the threefold symmetrical arrangement of the truncated elements of gp41 in their crystals (8, 67). Even this, however, may be viewed with some doubt. Frankel and Young (16) pointed out that the crystallographic structure may represent the fusion-active form of the gp41 oligomer that occurs upon binding of gp120 to the CD4 receptor. They make a persuasive argument, based on four lines of evidence, that the symmetric arrangement observed by X-ray crystallography may not exist in the free viral particle.

While it might be argued that AFM is simply not perceptive enough to resolve the symmetry of such molecular arrangements, in other studies (35–37, 41, 42, 55) AFM has been used to directly visualize symmetrical groupings of proteins on the surfaces of numerous virus particles, many of which are smaller than HIV.

The clusters of gp120 do not form spikes on the surface of HIV as is commonly described in the literature (3, 10). The

clusters are hardly protrusions at all. We suggest that the spikes observed by negative-staining electron microscopy may be an artifact of the penetration of heavy metal stain between envelope proteins. Indeed, the term "spike" appears to have assumed a rather imprecise, possibly misleading definition, and might best be used with caution. In the work of Briggs et al. (6), the spikes on the surfaces of HIV virions protruded about 7.5 nm, which is not inconsistent with the height above the virion surface that we observe by AFM for the tufts of protein. On the other hand, spikes of envelope protein are described on the surfaces of HFV that extend 13.8 nm above the surface (69), nearly twice the length of those on HIV. The gp41-gp 120 combination is probably better described as mushroom-shaped, with large, exposed exterior surfaces. The number of these gp120 clusters on individual virions, taken as the average from many particle images and assuming that one-third to one-half of the virus was visible, is close to 100 ± 20. This number is similar to that obtained by TEM (20) and the 70 to 140 trimers per virion estimated for simian immunodeficiency virus (9), but it is significantly greater than the 7 to 14 trimers per virion estimated for HIV by Chertova et al. (9). There is one complication, however, that could make our estimate somewhat problematic, and that is the quantity of host cell membrane proteins that may be incorporated into viral envelopes upon budding. If the amount is comparable to that of gp120, then substantially less of the gp120 could be present. That is, some of the protein tufts we observed might represent cellular proteins. It is not known whether virus envelope protein promotes exclusion of cellular proteins from the viral membrane, nor are there reliable estimates of the amount of cellular proteins generally incorporated. Examination of cell membranes from uninfected host cells by AFM, however, reveals a distribution of protein shapes and sizes that are far more diverse than we see on the more or less uniform surfaces of viruses. In particular, there is a much higher proportion of small proteins of <10 nm on normal cell surfaces. The appearance of the virus surfaces is not, in most respects, similar to host cell surfaces, and in particular, the many small proteins are lacking. Thus, we believe that the envelopes of the virions visualized by AFM are composed predominantly of gp120, with perhaps only occasional insertion of host cell proteins.

Our observation of anomalously small particles, both on glass substrates and on cell surfaces, suggests that some viruses may lack nucleic acid, or cores, and be otherwise empty. The very large virions of 160 to 240 nm in diameter are consistent with the findings of Gelderblom (20) and Briggs et al. (6) showing that as many as 30% of all virions may contain two or even three conical cores and that the diameters of these multicapsid virions are proportionately greater. The anomalously small and large particles, as well as the large variation of wild-type particle size about the mode of the distribution, suggest that virion size is a flexible property and is largely determined by the virion contents or the process of viral budding. Indeed, no two viral particles are likely to be exactly the same in either composition or structure. This is also the conclusion of Briggs et al. (6) based on entirely independent data.

Some AFM images suggest that the core of the virion can be expelled through a channel in the envelope surrounding it, as evidenced by the observed deep pit in some virions, though the explanation that these pits in fact represent a budding scar is also plausible. Indeed, such pits are observed by TEM after depletion of cholesterol from the virion by use of β-cyclodextrin (22).

Alternatively, the core may be lost by the splitting open of the virion, which only then falls apart in a piecemeal manner. From the thickness of the shells, or husks, which remain (about 35 nm), we conclude that they must include not only the lipid membrane and external envelope protein but the matrix protein on the interior of the membrane as well. This implies that the matrix protein is indeed firmly joined to the membrane and is physically contiguous with the envelope protein. This structure appears to be stable, as depletion of cholesterol from the membrane of HIV leads to disrupted virions from which the mature Gag proteins are lost but the envelope glycoproteins remain associated with a virion-like particle (22). Interestingly, matrix protein was lost with β-cyclodextrin treatment, further supporting the interpretation that myristoylated matrix protein remains associated with cholesterol found in both lipid rafts and the viral membrane.

Although adding little to the existing model of the virion, the appearance of extended protein-RNA complexes does confirm a few points. The nucleic acid is not naked but is tightly complexed with proteins, as evidenced by its obscurity in the presence of mild detergents and its appearance only when treated with SDS. The proteins are probably chiefly the nucleocapsid protein, as expected, but other, larger proteins or protein complexes are also bound to the nucleic acid. These could include the enzymes that are essential for replication.

The tight association that we observe between proteins and nucleic acid in the presence of detergents is consistent with the very positively charged nucleocapsid protein binding strongly to RNA. It would be difficult to argue that such interactions, with their condensing and organizing functions, do not also take place in the central lumens of immature particles and thereby facilitate alignment of uncleaved Gag polyproteins. This supports the hypothesis of both Briggs et al. (6) and Yeager et al. (73) that assembly of virus is likely to be a template-directed process driven by protein-nucleic acid interactions at the center of the particles.

From conventional negative-staining electron microscopy and, even more, from cryo-electron microscopy, it has become increasingly evident that maturation of retroviral particles is accompanied by a dramatic redistribution of components and vast internal structural rearrangement (6, 17, 70, 73). This is brought about by HIV protease cleavage of the Gag proteins. There is no indication from previous analyses, however, that this produces any change in the size or the external appearance of the virions. Our experiments with virus infection in the presence of protease inhibitors are entirely consistent with those investigations. We also find no significant change in virion diameter when mature and immature particles are compared, nor do we find any perceptible change in their external appearance.

ACKNOWLEDGMENTS

We thank Aaron Greenwood for assistance with the preparation of figures.

This research was supported by a contract from NASA and a grant from the NIH and in part by a grant from the California University-Wide Biotechnology Training program (J.G.V.). W.E.R. is a Burroughs-Wellcome Fund Clinical Scientist in Translational Research.

REFERENCES

1. **Baker, T. S., N. H. Olson, and S. D. Fuller.** 1999. Adding the third dimension to virus life cycles: three-dimensional reconstruction of icosahedral viruses from cryo-electron micrographs. Microbiol. Mol. Biol. Rev. **63:**862–922.
2. **Bennett, V.** 1982. The molecular basis for membrane-cytoskeleton association in human erythrocytes. J. Cell. Biochem. **18:**49–65.
3. **Berger, E. A.** 1998. And the best picture is—the HIV gp envelope, please! Nat. Struct. Biol. **5:**671–674.
4. **Bolognesi, D. P., R. C. Montelaro, H. Frank, and W. Schafer.** 1978. Assembly of C-type oncornaviruses. A model. Science **199:**183–186.
5. **Braet, F., D. Vermijlen, V. Bossuyt, R. De Zanger, and E. Wisse.** 2001. Early detection of cytotoxic events between hepatic natural killer cells and colon carcinoma cells as probed with the atomic force microscope. Ultramicroscopy **89:**265–273.
6. **Briggs, J. A. G., T. Wilk, R. Welker, H.-G. Krausslich, and S. D. Fuller.** 2003. Structural organization of authentic, mature HIV-1 virions and cores. EMBO J. **22:**1707–1715.
7. **Bustamante, C., and D. Keller.** 1995. Scanning force microscopy in biology. Phys. Today **48:**32–38.
8. **Chan, D. C., J. M. Fass, E. A. Berger, and P. S. Kim.** 1997. Core structure of gp41 from the HIV envelope glycoprotein. Cell **89:**263–273.
9. **Chertova, E., J. W. Bess, Jr., B. J. Crise, R. C. Sowder II, T. M. Schaden, J. M. Hilburn, J. A. Hoxie, R. E. Benveniste, J. D. Lifson, L. E. Henderson, and L. O. Arthur.** 2002. Envelope glycoprotein incorporation, not shedding of surface envelope glycoprotein (gp120/SU), is the primary determinant of SU content of purified human immunodeficiency virus type 1 and simian immunodeficiency virus. J. Virol. **76:**5315–5325.
10. **Coffin, J. M., S. H. Hughes, and H. E. Varmus (ed.).** 1997. Retroviruses. Cold Spring Harbor Laboratory Press, Cold Spring Harbor, N.Y.
11. **Craven, R. C., and L. J. Parent.** 1996. Dynamic interactions of the Gag polyprotein. Curr. Top. Microbiol. Immunol. **214:**65–94.
12. **Demirov, D. G., A. Ono, J. M. Orenstein, and E. O. Freed.** 2002. Overexpression of the N-terminal domain of TSG101 inhibits HIV-1 budding by blocking late domain function. Proc. Natl. Acad. Sci. USA **99:**955–960.
13. **Demirov, D. G., J. M. Orenstein, and E. O. Freed.** 2002. The late domain of human immunodeficiency virus type 1 p6 promotes virus release in a cell type-dependent manner. Virology **76:**105–117.
14. **Donnadieu, E., V. Lang, G. Bismuth, W. Ellmeier, O. Acuto, F. Michel, and A. Trautmann.** 2001. Differential roles of Lck and Itk in T cell response to antigen recognition revealed by calcium imaging and electron microscopy. J. Immunol. **166:**5540–5549.
15. **Fass, D. R., R. A. Davey, C. A. Hamson, P. S. Kim, J. M. Cunningham, and J. M. Berger.** 1997. Structure of a murine leukemia virus receptor-binding glycoprotein at 2.0 angstrom resolution. Science **277:**1662–1666.
16. **Frankel, A. D., and J. A. T. Young.** 1998. HIV-1: fifteen proteins and an RNA. Annu. Rev. Biochem. **67:**1–25.
17. **Fuller, S. D., T. Wilk, B. E. Gown, H.-G. Krausslich, and V. M. Vogt.** 1997. Cryo-electron microscopy reveals ordered domains in the immature HIV-1 particle. Curr. Biol. **7:**729–738.
18. **Ganser, B. K., S. Li, V. Y. Klishko, J. T. Finch, and W. I. Sundquist.** 1999. Assembly and analysis of conical models for the HIV-1 core. Science **283:**80–82.
19. **Garrus, J. E., U. K. von Schwedler, O. W. Pornillos, S. G. Morham, K. H. Zavitz, H. E. Wang, D. A. Wettstain, K. M. Stray, M. Cote, R. L. Rich, D. G. Myszka, and W. I. Sundquist.** 2001. Tsg101 and the vacuolar protein sorting pathway are essential for HIV-1 budding. Cell **107:**55–65.
20. **Gelderblom, H. R.** 1991. Assembly and morphology of HIV: potential effect of structure on viral function. AIDS **5:**617–637.
21. **Gelderblom, H. R., H. Reuphe, T. Winkel, R. Kunze, and G. Pauli.** 1987. MHC-antigens: constituents of the envelopes of human and simian immunodeficiency virus. Z. Naturforsch. Sect. C **42:**1328–1334.
22. **Graham, D. R. M., E. Chertova, J. M. Hilburn, L. O. Arthur, and J. E. Hildreth.** 2003. Cholesterol depletion of human immunodeficiency virus type 1 and simian immunodeficiency virus with β-cyclodextrin inactivates and permeabilizes the virions: evidence for virion-associated lipid rafts. J. Virol. **77:**8237–8248.
23. **Grewe, C., A. Beck, and H. R. Gelderblom.** 1990. HIV: early virus-cell interactions. J. Acquir. Immun. Defic. Syndr. **3:**965–974.
24. **Hansma, H. G., K. J. Kim, D. E. Laney, R. A. Garcia, M. Argaman, M. J. Allen, and S. M. Parsons.** 1997. Properties of biomolecules measured from atomic force microscope images: a review. J. Struct. Biol. **119:**99–108.
25. **Hartwig, J. H., and M. DeSisto.** 1991. The cytoskeleton of the resting human blood platelet: structure of the membrane skeleton and its attachment to actin filaments. J. Cell Biol. **112:**407–425.
26. **Henderson, L. E., H. C. Krutzsch, and S. Oroszlan.** 1983. Myristyl amino-terminal acylation of murine retrovirus proteins: an unusual post-translational protein modification. Proc. Natl. Acad. Sci. USA **80:**339–343.
27. **Hill, C. P., D. Worthylake, D. P. Bancroft, A. M. Christensen, and W. I. Sundquist.** 1996. Crystal structures of the trimeric human immunodeficiency virus type 1 matrix protein: implications for membrane association and assembly. Proc. Natl. Acad. Sci. USA **93:**3099–3104.
28. **Hockley, D. J., M. V. Nermut, C. Grief, J. B. Jowett, and I. M. Jones.** 1994. Comparative morphology of Gag protein structures produced by mutants of the gag gene of human immunodeficiency virus type 1. J. Gen. Virol. **75:**2985–2987.
29. **Hogland, S., L. G. Ofverstedt, A. Nilson, H. Lundquist, H. R. Gelderblom, M. Ozel, and U. Skoglund.** 1992. Spatial visualization of the maturing HIV-1 core and its linkage to the envelope. AIDS Res. Hum. Retrovir. **8:**1–7.
30. **Huang, Y., J. Mak, Q. Cao, Z. Liz, M. A. Wainberg, and L. Kleiman.** 1994. Incorporation of excess wild-type and mutant tRNA(2Lys) into human immunodeficiency virus type 1. J. Virol. **68:**7676–7683.
31. **Jiang, M., J. Mak, A. Ladha, E. Cohen, M. Klein, B. Rovinski, and L. Kleiman.** 1993. Identification of tRNAs incorporated into wild-type and mutant human immunodeficiency virus type 1. J. Virol. **67:**3246–3253.
32. **King, P. J., and W. E. Robinson, Jr.** 1998. Resistance to the anti-human immunodeficiency virus type 1 compound L-chicoric acid results from a single mutation at amino acid 140 of integrase. J. Virol. **72:**8420–8424.
33. **Kotov, A., J. Zhou, P. Flicker, and C. Aiken.** 1999. Association of Nef with the human immunodeficiency virus type 1 core. J. Virol. **73:**8824–8830.
34. **Kuznetsov, Y. G., S. Datta, N. H. Kothari, A. Greenwood, H. Fan, and A. McPherson.** 2002. Atomic force microscopy investigation of fibroblasts infected with wild type and mutant murine leukemic virus (MuLV). Biophys. J. **83:**3665–3674.
35. **Kuznetsov, Y. G., A. J. Malkin, R. W. Lucas, and A. McPherson.** 2000. Atomic force microscopy studies of icosahedral virus crystal growth. Colloids Surf. B Biointerfaces **19:**333–346.
36. **Kuznetsov, Y. G., A. J. Malkin, R. W. Lucas, M. Plomp, and A. McPherson.** 2001. Imaging of viruses by atomic force microscopy. J. Gen. Virol. **82:**2025–2034.
37. **Kuznetsov, Y. G., A. J. Malkin, and A. McPherson.** 1997. Atomic force microscopy studies of living cells: visualization of motility, division, aggregation, transformation, and apoptosis. J. Struct. Biol. **120:**180–191.
38. **Kwong, P. D., R. Wyatt, J. Robinson, R. W. Sweet, J. Sodroski, and W. A. Hendrickson.** 1998. Structure of an HIV gp120 envelope glycoprotein in complex with the CD4 receptor and a neutralizing human antibody. Nature **393:**648–659.
39. **Lee, Y.-M., and X. F. Yu.** 1998. Identification and characterization of virus assembly intermediate complexes in HIV-1-infected CD4+ T cells. Virology **243:**78–93.
40. **Liao, Z., L. M. Cimakasky, R. Hampton, D. H. Nguyen, and J. E. Hildreth.** 2001. Lipid rafts and HIV pathogenesis: host membrane cholesterol is required for infection by HIV type 1. AIDS Res. Hum. Retrovir. **17:**1009–1019.
41. **Lucas, R. W., Y. G. Kuznetsov, S. B. Larson, and A. McPherson.** 2001. Crystallization of Brome mosaic virus and T=1 Brome mosaic virus particles following a structural transition. Virology **286:**290–303.
42. **Malkin, A. J., Y. G. Kuznetsov, R. W. Lucas, and A. McPherson.** 1999. Surface processes in the crystallization of turnip yellow mosaic virus visualized by atomic force microscopy. J. Struct. Biol. **127:**35–43.
43. **Malkin, A. J., A. McPherson, and P. D. Gershon.** 2003. Structure of intracellular mature vaccinia virus visualized by in situ AFM. J. Virol. **77:**6332–6340.
44. **Martin-Serrano, J., T. Zang, and P. D. Bieniasz.** 2003. Role of ESCRT-1 in retroviral budding. Virology **77:**4794–4804.
45. **Momany, C., L. C. Kovari, A. J. Prongay, W. Keller, R. K. Gitti, B. M. Lee, A. E. Gorbaleny, L. Tong, J. McClure, L. S. Ehrlich, M. F. Summers, C. Carter, and M. G. Rossmann.** 1996. Crystal structure of dimeric HIV-1 capsid protein. Nat. Struct. Biol. **3:**763–771.
46. **Moore, J. P.** 1997. Coreceptors: implications for HIV pathogenesis and therapy. Science **276:**51–52.
47. **Morikawa, Y., M. Shibuya, T. Gotoa, and K. Sano.** 2000. In vitro processing of human immunodeficiency virus type 1 gag virus-like particles. Virology **272:**366–374.
48. **Morris, V. J.** 1994. Biological applications of scanning probe microscopies. Prog. Biophys. Mol. Biol. **61:**131–185.
49. **Neagu, C., K. O. Vanderwerf, C. A. J. Putman, Y. M. Kraan, B. G. Degrooth, N. F. Vanhulst, and J. Greve.** 1994. Analysis of immunolabeled cells by atomic force microscopy, optical microscopy, and flow cytometry. J. Struct. Biol. **112:**32–40.
50. **Nermut, M. V., C. Grief, S. Haskmi, and D. J. Hockley.** 1993. Further evidence of icosahedral symmetry in human and simian immunodeficiency virus. AIDS Res. Hum. Retrovir. **9:**929–938.
51. **Nguyen, D. H., and J. K. Hildreth.** 2000. Evidence for budding of human immunodeficiency virus type 1 selectively from glycolipid-enriched membrane lipid rafts. J. Virol. **74:**3264–3272.
52. **Ott, D. E., L. V. Coren, D. G. Johnson, R. C. Sowder II, L. O. Arthur, and L. E. Henderson.** 1995. Analysis and localization of cyclophilin A found in the virions of human immunodeficiency virus type 1 MN strain. AIDS Res. Hum. Retrovir. **11:**1003–1006.
53. **Parker, S. D., J. S. Wall, and E. Hunter.** 2001. Analysis of Mason-Pfizer monkey virus Gag particles by scanning transmission electron microscopy. J. Virol. **75:**9543–9548.
54. **Perotti, M. E., X. Tan, and D. M. Phillips.** 1996. Directional budding of human immunodeficiency virus from monocytes. Virology **70:**5916–5921.

55. **Plomp, M., M. K. Rice, E. K. Wagner, A. McPherson, and A. J. Malkin.** 2002. Rapid visualization at high resolution of pathogens by atomic force microscopy: structural studies of herpes simplex virus-1. Am. J. Pathol. **160:**1959–1966.
56. **Pornillos, O. W., S. L. Alam, R. L. Rich, D. G. Myszka, D. R. Davis, and W. I. Sundquist.** 2002. Structure and functional interactions of the Tsg101 UEV domain. EMBO J. **21:**2397–2406.
57. **Pralle, A., P. Keller, E. L. Florin, K. Simons, and J. K. H. Horber.** 2000. Sphingolipid-cholesterol rafts diffuse as small entities in the plasma membrane of mammalian cells. J. Cell Biol. **148:**997–1007.
58. **Rein, A., M. R. McClure, N. R. Rice, R. B. Luftig, and A. M. Schultz.** 1986. Myristylation site in Pr65 Gag is essential for virus particle formation by Moloney murine leukemia virus. Proc. Natl. Acad. Sci. USA **83:**7246–7250.
59. **Robinson, W. E., Jr., D. C. Montefiori, D. H. Gillespie, and W. M. Mitchell.** 1989. Complement-mediated, antibody-dependent enhancement of human immunodeficiency virus type 1 (HIV-1) infection in vitro increases HIV-1 RNA and protein synthesis and infectious virus production. J. Acquir. Immun. Defic. Syndr. **2:**33–42.
60. **Sakaue, M., and K. Taniguchi.** 2001. Imaging of the lectin-labeled cell surface of human lymphocytes by the use of atomic force microscope. J. Vet. Med. Sci. **63:**223–225.
61. **Schutz, G. J., G. Kada, V. P. Pastushenko, and H. Schindler.** 2000. Properties of lipid microdomains in the muscle cell membrane visualized by single molecule microscopy. EMBO J. **19:**892–901.
62. **Shibata-Seki, T., W. Watanabe, and J. Masai.** 1994. Imaging of cells with atomic force microscopy operating at a "tapping mode." J. Vac. Sci. Technol. B **12:**1530–1534.
63. **Shiraishi, T.** 2001. Myristoylation of human immunodeficiency virus type 1 gag protein is required for efficient env protein transportation to the surface of cells. Biochem. Biophys. Res. Commun. **282:**1201–1205.
64. **Turner, B. G., and M. F. Summers.** 1999. Structural biology of HIV. J. Mol. Biol. **285:**1–32.
65. **Varma, R., and S. Mayor.** 1998. GPI-anchored proteins are organized in submicron domains at the cell surface. Nature **394:**798–801.
66. **Vogt, V. M.** 1997. Retroviral virions and genomes, p. 27–69. *In* J. M. Coffin, S. H. Hughes, and H. E. Varmus (ed.), Retroviruses, vol. 1. Cold Spring Harbor Laboratory Press, Cold Spring Harbor, N.Y.
67. **Weissenhorn, W., A. Dessen, S. C. Harrison, J. J. Skehel, and D. C. Wiley.** 1997. Atomic structure of the ectodomain from HIV-1 gp41. Nature **387:**426–430.
68. **Weldon, R. A., and E. Hunter.** 1997. Molecular requirements for retrovirus assembly, p. 280. *In* W. Chin, R. M. Burnett, and R. L. Garcea (ed.), Structural biology of viruses. Oxford University Press, Oxford, United Kingdom.
69. **Wilk, T.** 2000. The intact retroviral Env glycoprotein of human foamy virus is a trimer. J. Virol. **74:**2885–2891.
70. **Wilk, T., I. Gross, B. E. Gowen, T. Rutten, D. H. Felix, R. Welker, H.-G. Krausslich, P. Boulanger, and S. D. Fuller.** 2001. Organization of immature human immunodeficiency virus type 1. J. Virol. **75:**759–771.
71. **Wyatt, R., and J. Sodroski.** 1998. The HIV-1 envelope glycoproteins: fusogens, antigens and immunogens. Science **280:**1884–1888.
72. **Wyma, D. J., A. Kotov, and C. Aiken.** 2000. Evidence for a stable interaction of gp41 with $Pr55^{Gag}$ in immature human immunodeficiency virus type 1 particles. J. Virol. **74:**9381–9387.
73. **Yeager, M., E. M. Wilson-Kubalek, S. G. Weiner, P. O. Brown, and A. Rein.** 1998. Supramolecular organization of immature and mature murine leukemia virus revealed by electron cryo-microscopy: implications for retroviral assembly mechanisms. Proc. Natl. Acad. Sci. USA **95:**7299–7304.